

# The effect and mechanism of SHP2 on sepsis induced myocardial injury via modulating Src/ERK-autophagy signal

Jie Wang<sup>1</sup>, Qian Jia<sup>2</sup>, Yu Zhang<sup>1</sup>, Jing Li<sup>1</sup>

<sup>1</sup>Department of Clinical Laboratory, Hebei General Hospital, Shijiazhuang 050051, Hebei, China

<sup>2</sup>Medical Examination Center, Hebei General Hospital, Shijiazhuang 050051, Hebei, China

**Correspondence to:** Jie Wang; email: [wangjie7946852@163.com](mailto:wangjie7946852@163.com), <https://orcid.org/0000-0003-1520-5802>

**Keywords:** SHP2, sepsis, myocardial injury, apoptosis, oxidative stress

**Received:** July 7, 2023

**Accepted:** January 24, 2024

**Published:** February 23, 2024

**Copyright:** © 2024 Wang et al. This is an open access article distributed under the terms of the [Creative Commons Attribution License](https://creativecommons.org/licenses/by/4.0/) (CC BY 4.0), which permits unrestricted use, distribution, and reproduction in any medium, provided the original author and source are credited.

## ABSTRACT

**Objective:** To investigate the effect and mechanism of SHP2 on myocardial injury induced by sepsis.

**Methods:** The cardiac function of mice was examined by echocardiography, the myocardial pathological changes of mice were detected by HE staining, the ultrastructural changes of mice myocardial cells were examined by transmission electron microscopy, and the expression of p-SHP2, p-Src, p-ERK1/2, oxidative stress related proteins and apoptosis related proteins of mice myocardial cells were detected by Western blot. Moreover, apoptosis of cardiomyocytes was detected by TUNEL staining.

**Results:** The cardiac function of model group mice was better than that of PHPS1 group, but poorer than that of sham group. The pathological changes and ultrastructural changes of myocardium of mice in model group were better than those in PHPS1 group, and no changes was found in sham group. The expression of p-SHP2 protein in model group mice was higher than that in PHPS1 group and sham group, but the expression of p-Src, p-ERK1/2, oxidative stress related protein and apoptosis related protein were lower than that in PHPS1 group while higher than that in sham group. The addition of PHPS1 inhibited the expression of p-SHP2 and increased the expression of p-Src, oxidative stress-related proteins and apoptosis-related proteins. However, the gap in the expression levels of oxidative stress-related proteins and apoptosis-related proteins narrowed with the addition of NAC.

**Conclusions:** SHP2 can ameliorate myocardial injury induced by sepsis by inhibiting oxidative stress-mediated cardiomyocyte apoptosis through Src/ERK pathway.

## INTRODUCTION

Sepsis epitomizes a complex condition of multi-organ failure precipitated by infection, manifesting with alarming frequency and a concomitant high mortality globally [1, 2]. A frequent sequela of sepsis is myocardial compromise, hallmarked by impairment of cardiac contractility and compliance [3]. Approximately half of those afflicted by sepsis exhibit myocardial distress, facing a prognostic outlook considerably grimmer than their counterparts without cardiac implications [4].

The pathological landscape of sepsis-induced myocardial compromise is multifaceted [5]. Of the myriad contributors, oxidative stress is increasingly recognized as a pivotal driver of both the emergence and progression of cardiac injury in sepsis [6]. Sepsis inflicts substantial mitochondrial harm within cardiac cells, culminating in the prolific generation of reactive oxygen species and a surge in oxidative strain [7]. The deleterious effects of oxidative stress extend beyond the diminishment of cardiomyocyte contractility; they decisively cripple the myocardium's aptitude for efficacious blood circulation. In its most devastating

form, oxidative stress orchestrates the apoptotic demise of cardiomyocytes [8–10].

SHP2, a ubiquitously expressed non-receptor protein tyrosine phosphatase, encoded by the PTPN11 locus, is integral to intracellular signaling circuits and the regulation of cellular vitality, proliferation, and motility [11, 12]. Empirical evidence suggests that the retention of SHP2 activity harbors therapeutic promise in the context of sepsis, while its activation has been shown to stifle ROS generation [13, 14]. Research illuminates how cytokine-evoked ROS generation during sepsis leads to SHP2 inactivation, thus exacerbating endothelial inflammatory responses [13]. Furthermore, overexpression of Src homology-2 domain-containing protein tyrosine phosphatase 2 has been noted in macrophages and pulmonary tissue amid sepsis, activating the SHP2-associated MAPK pathway through lipopolysaccharide stimulation. Ablation of the SHP2 gene subverts the lipopolysaccharide-provoked inflammation and phosphorylation of regulatory elements within the macrophage NF- $\kappa$ B axis, thereby mitigating acute pulmonary damage. Evidence also posits that SHP2 inhibition ameliorates acute renal injury prompted by the Hem/CLP bidirectional assault model, potentially through its anti-inflammatory efficacy in tempering Erk1/2 and STAT3 pathway activation [14–17]. Nevertheless, the mechanisms underpinning SHP2's involvement in sepsis-induced myocardial injury remain shrouded in obscurity. Against this backdrop, we used *in vivo* and *in vitro* experiments in this study to explore the effect and mechanism of SHP2

on myocardial injury in sepsis, and provide new therapeutic ideas and targets for myocardial injury in sepsis.

## RESULTS

### Mouse ultrasound electrocardiogram results

The results of echocardiography showed that compared with the sham group, the LVEF, LVFS and E/A of the mice in the model group and PHPS1 group were significantly decreased, while the LVEF, LVFS and E/A of the mice in the PHPS1 group were significantly decreased compared with the model group (Figure 1). The results showed that SHP2 could significantly improve cardiac dysfunction caused by myocardial injury in sepsis.

### Results of HE staining in mice myocardium

The results of HE staining showed that the myocardial cells of the sham group were arranged orderly, and no pathological damage such as necrosis, hyperemia and edema was found. In the model group, the arrangement of myocardial cells was disordered, with rupture of sarcolemmal membrane and enlargement of nucleus, accompanied by slight necrosis, interstitial hyperemia, edema and infiltration of inflammatory cells. Compared with the model group, the arrangement of cardiomyocytes in the PHPS1 group was disordered, and the conditions of nuclear necrosis, interstitial hyperemia and inflammatory cell infiltration were significantly worse

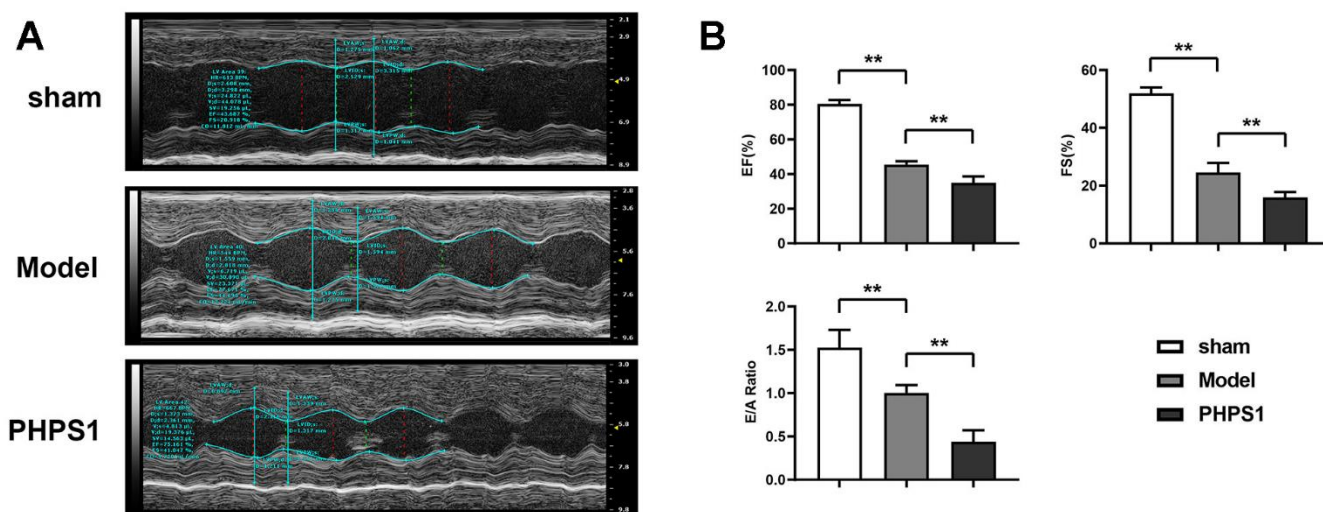


**Figure 1. Ultrasound electrocardiogram examination results of mice in each group.** (A) Left ventricular echocardiography of mice; (B) Statistical results of LVEF, LVFS, E/A ratios of left ventricle in mice, data was presented as  $X \pm S$ . Comparisons between sham group and model group,  $**p < 0.01$ ; Comparisons between sham group and PHPS1 group,  $**p < 0.01$ ; Comparisons between model group and PHPS1 group,  $**p < 0.01$ .

(Figure 2), turning out that SHP2 can ameliorate myocardial pathology caused by myocardial injury caused by sepsis.

### Results of transmission electron microscopy of mouse cardiomyocytes

The results of transmission electron microscope indicated that the myocardial fibers of mice in sham group were arranged in order, the mitochondrial cristae was tight, the mitochondrial double membrane was not damaged, without dissolution, vacuole and other phenomena, the autophagy phenomenon was weak, and the number of lysosomes was less; In model group, the myocardial fibers were broken, the sarcomere was arranged disorderly, some mitochondria were swollen and broken, vacuolated, the ridge structure was disordered, and the number of autophagy bodies and lysosomes increased. In the PHPS1 group, severe myocardial fiber rupture was severe, sarcomere arrangement disorder was aggregated, a large number of mitochondria swelling and rupture was present, vacuolation, ridge structure was disorder, autophagy body and lysosome increased significantly (Figure 3). It indicated that SHP2 could mitigate the ultrastructural changes of myocardial cells induced by sepsis.

### Results of the detection of p-SHP2, p-Src and p-ERK proteins in mice cardiomyocytes

The western blot results showed that the relative protein expressions of p-Src and p-ERK1/2 in the sham operation group were significantly lower than those in the model group and PHPS1 group, while the relative protein expressions of p-Src and p-ERK1/2 in the

PHPS1 group were significantly higher than those in the model group. Compared with the sham operation group, the relative protein expression of p-SHP2 in the model group was significantly increased, and the relative protein expression of p-SHP2 in the PHPS1 group was significantly decreased (Figure 4). These results showed that SHP2 could suppress the protein activity of Src and ERK in myocardial injury induced by sepsis.

### Results of oxidative stress related proteins in mouse cardiomyocytes

The results of western blot showed that the relative protein expressions of P22, P47 and gp91 in the model group and PHPS1 group were significantly increased compared with the sham group. Compared with the model group, the relative protein expressions of P22, P47 and gp91 in the PHPS1 group were significantly increased (Figure 5), which indicated that SHP2 could improve the production of oxidative stress in sepsis induced myocardial injury.

### Results of the apoptosis-related proteins and the apoptosis of cells

Western blotting results showed that the relative protein expressions of Bax, sheared caspase-3 and sheared caspase-12 in the model group and PHPS1 group were significantly increased compared with the sham group. Compared with the model group, the relative protein expressions of Bax, cleaved-caspase-3 and cleaved-caspase-12 in the PHPS1 group were significantly increased. The results of TUNEL assay showed that the number of apoptotic cells in the model

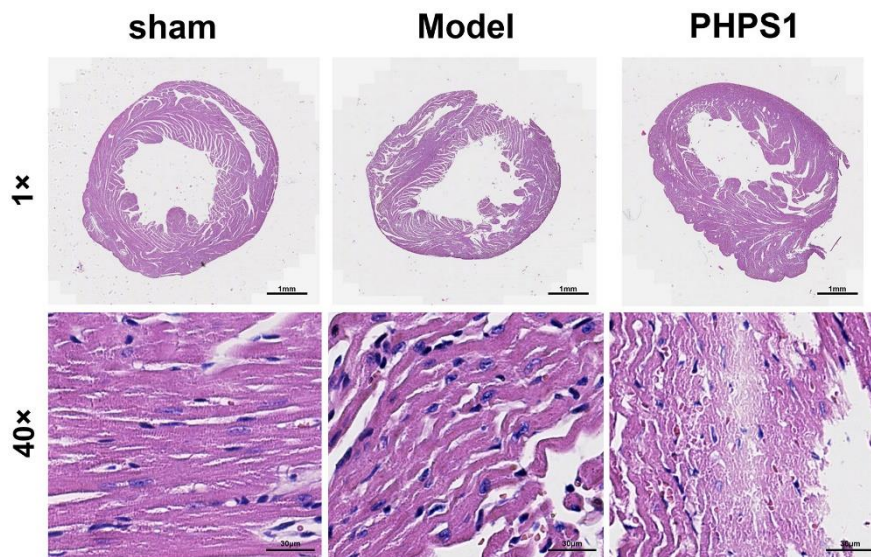


Figure 2. HE staining results of myocardium in mice of each group.

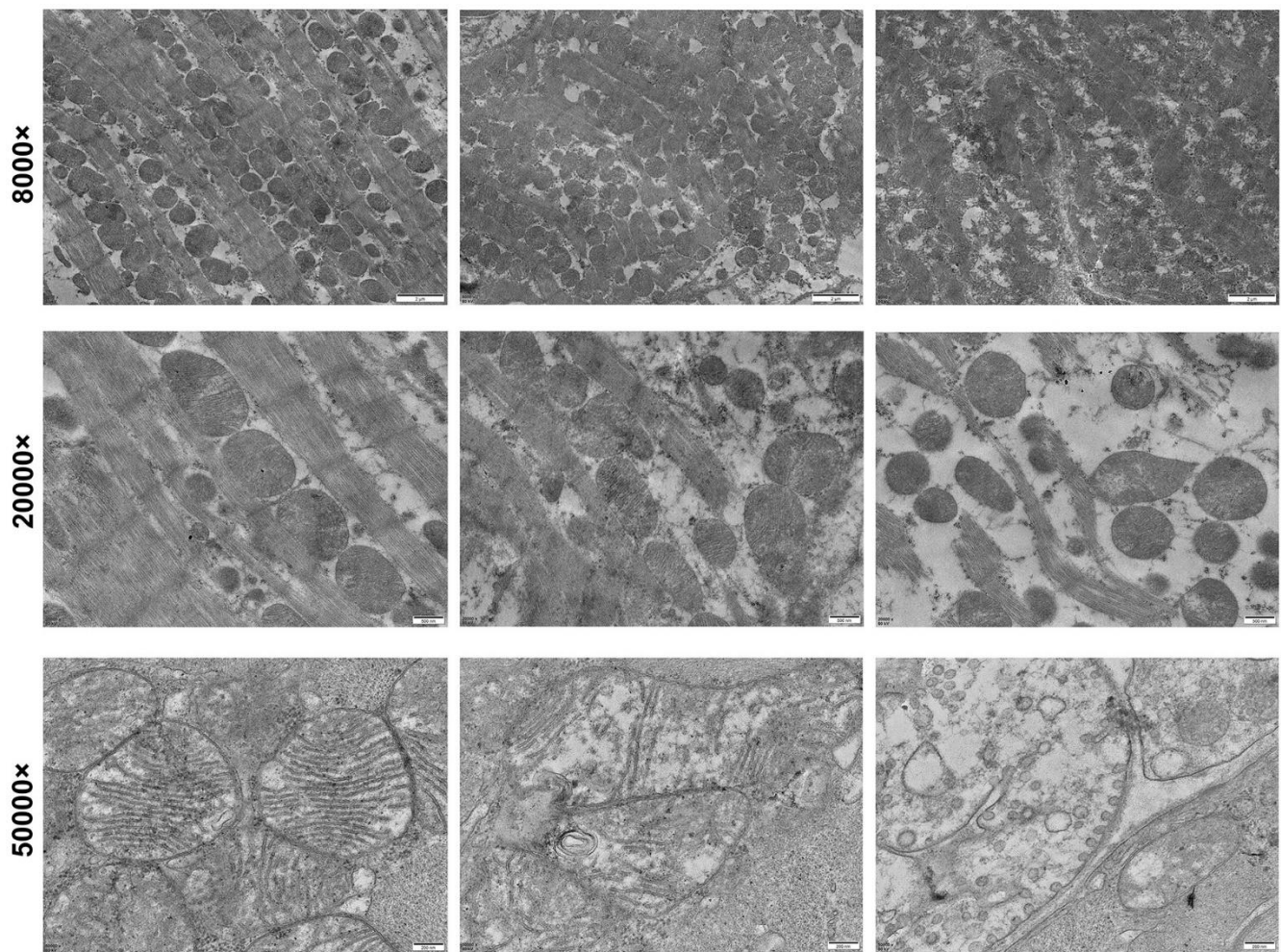


Figure 3. Transmission electron microscopic examination of myocardial cells in each group.

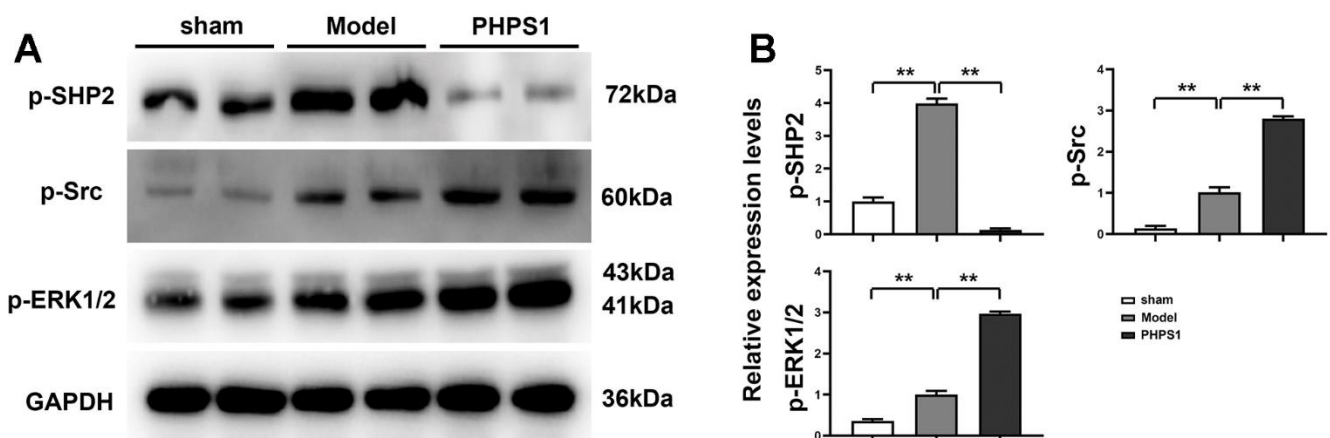


Figure 4. Western blot results of p-SHP2, p-Src and p-ERK protein in myocardial cells of mice in each group. (A) Western blot results of p-SHP2, p-Src and p-ERK1/2 in mouse cardiomyocytes in each group; (B) Statistical diagram of the expression levels of p-SHP2, p-Src and p-ERK1/2 proteins in mouse cardiomyocytes in each group, and the data was shown as X±S. Comparisons between sham group and model group, \*\*p<0.01; Comparisons between sham group and PHPS1 group, \*\*p<0.05; Comparisons between model group and PHPS1 group, \*\*p<0.01.

group and PHPS1 group was significantly higher than that in the sham group. Compared with the model group, the number of apoptotic cells in the PHPS1 group was significantly increased (Figure 6). The results manifested that SHP2 inhibited cardiomyocyte apoptosis in septic myocardial injury.

### ***In vitro* experimental results**

Western blot results showed that the expression of p-SHP2 protein in Group c was lower than that in Group b, but the expression level of p-Src, P22, P47, Bax and Caspase-3 protein in Group c was higher than that in Group b. The expression of p-SHP2 protein in Group d was higher than that in Group e, but the expression of p-Src protein was lower than that in Group c. The differences between the relative protein expressions of P22, P47, Bax, and cleaved-caspase-3 were all narrowed between groups d and e after the addition of the antioxidant NAC (Figure 7). These results suggested that SHP2 inhibited the apoptosis of cardiomyocytes induced by oxidative stress in septic myocardial injury by inhibiting Src/ERK pathway (Figure 8).

## **DISCUSSION**

Myocardial damage, as a significant complication of sepsis, substantially elevates patient mortality [18]. The precise mechanism underlying sepsis-induced myocardial damage remains inadequately understood [19]. Current approaches to treating myocardial injury in sepsis involve the use of vasopressors, dobutamine, levosimendan, ivabradine, and mechanical support [20]. However, these therapies have not proven to be optimal in clinical practice primarily due to the incomplete

elucidation of the molecular mechanisms underlying myocardial injury in sepsis [21, 22]. Nonetheless, there is a prevailing belief that oxidative stress plays a role in the pathological process of sepsis-induced myocardial injury, and its inhibition is considered beneficial for ameliorating the condition [23].

SHP2 is a widely expressed cytoplasmic tyrosine phosphatase featuring two SH2 domains and a catalytic protein tyrosine phosphatase (PTP) domain [24]. It exerts a pivotal role in growth factor and cytokine signaling, as well as extracellular matrix receptor-mediated cellular proliferation, differentiation, migration, and survival [25]. Furthermore, PHPS1 serves as a potent cell-permeable inhibitor with specific inhibitory effects on SHP2 [26]. In this investigation, intervention in three groups of mice revealed that the left ventricular ejection fraction (LVEF), left ventricular fractional shortening (LVFS), and E/A ratios of mice in the model group were higher than PHPS1 group, indicative of SHP2 significantly ameliorating cardiac dysfunction resulting from septic myocardial injury. Meanwhile, compared to the sham group administered normal saline, the myocardial cells in the model group exhibited disordered arrangement, ruptured sarcolemma, enlarged nuclei, accompanied by necrosis, interstitial congestion and edema, inflammatory cell infiltration, as well as mitochondrial destruction and appearance of autophagic bodies. The situation in the PHPS1 group was even more severe. The presence of autophagosomes in the findings was attributed to the fact that ROS not only directly triggers apoptosis but also induces apoptosis by instigating autophagy [27]. These outcomes further corroborate the significant inhibitory effect of SHP2 on the myocardial pathological and ultrastructural changes induced by sepsis.

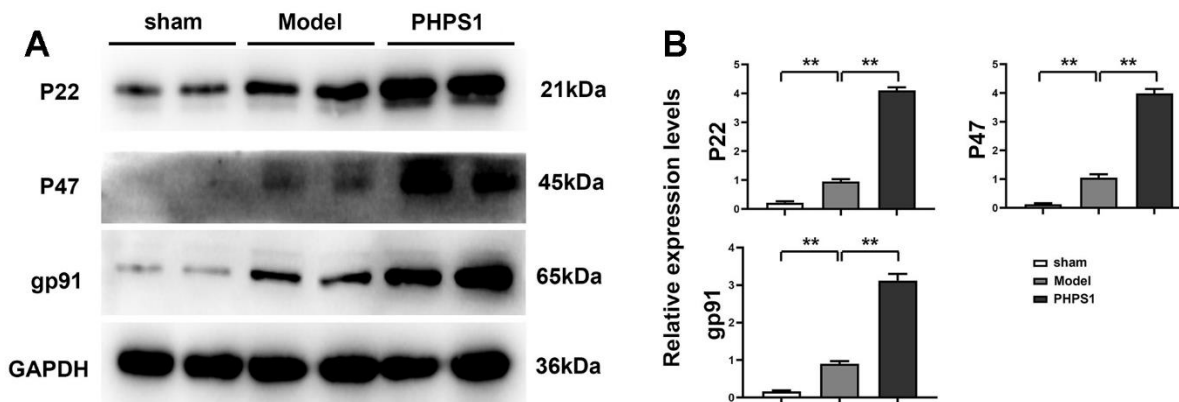


**Figure 5. Western blot results of oxidative stress related proteins in myocardial cells of mice in each group. (A)** Western blot results of P22, P47 and gp91 in mouse cardiomyocytes in each group; **(B)** Statistical plots of P22, P47 and gp91 expression levels in mice cardiomyocytes in each group, and the data was shown as  $X \pm S$ . Comparisons between sham group and model group,  $**p < 0.01$ ; Comparisons between sham group and PHPS1 group,  $**p < 0.01$ ; Comparisons between model group and PHPS1 group,  $**p < 0.01$ .

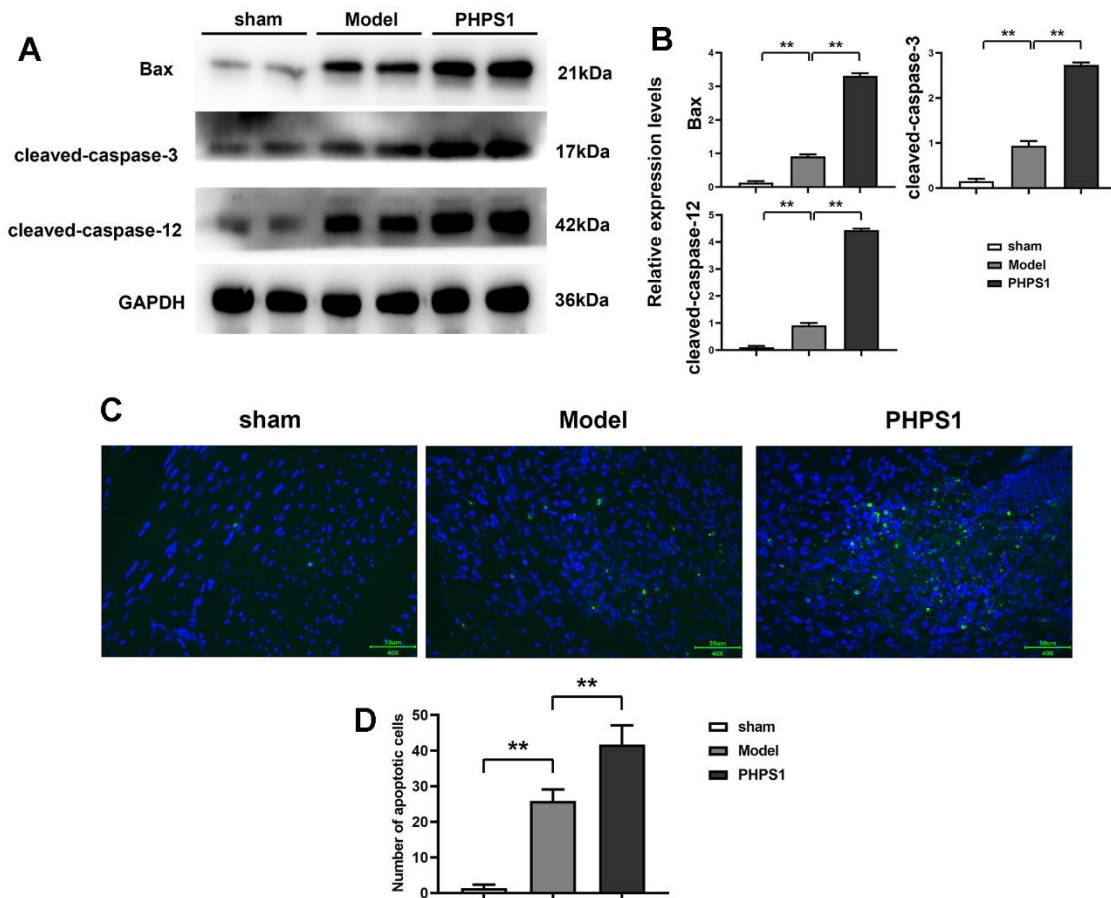


**Figure 6. Results of the expression of apoptosis-related proteins in mouse cardiomyocytes and the cell apoptosis condition.** (A) Western blot results of Bax, cleaved-Caspase-3 and cleaved-Caspase-12 in mouse cardiomyocytes in each group; (B) Statistical plot of Bax, cleaved-Caspase-3 and cleaved-Caspase-12 expression levels in mouse cardiomyocytes in each group; (C) Plot of TUNEL assay results; (D) Apoptotic cell count statistics, data was shown as  $X \pm S$ . Comparisons between sham group and model group,  $**p < 0.01$ ; Comparisons between sham group and PHPS1 group,  $**p < 0.01$ ; Comparisons between model group and PHPS1 group,  $**p < 0.01$ .

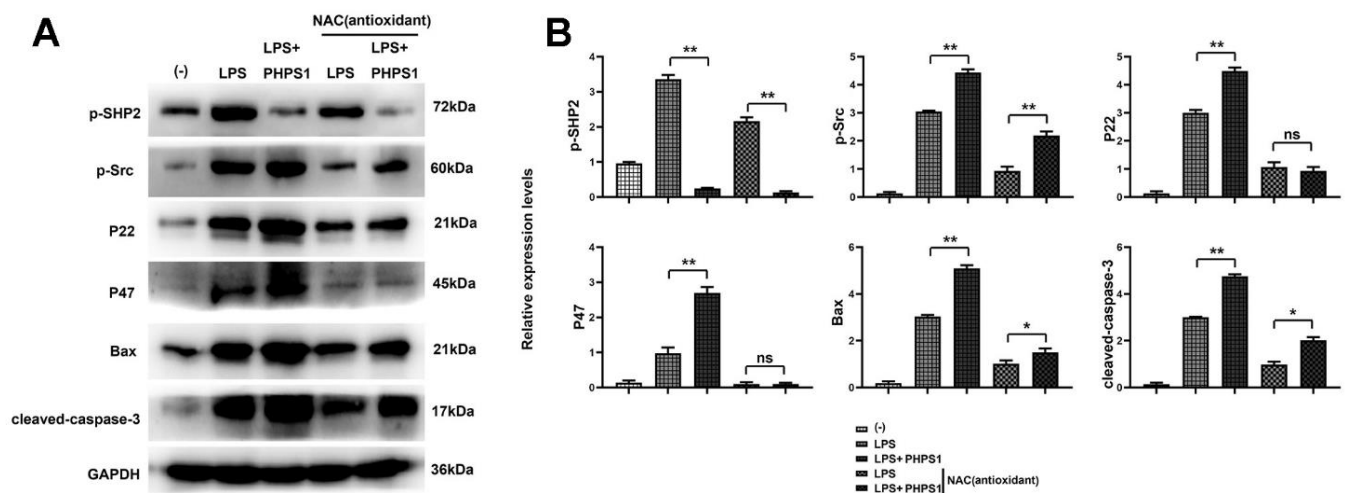


**Figure 7. In vitro experiment results.** (A) Western blot results plots of p-SHP2, p-Src, P22, P47, Bax, and cleaved-Caspase-3; (B) Statistical plots of p-SHP2, p-Src, P22, P47, Bax, and cleaved-Caspase-3 expression levels, the data was shown as  $X \pm S$ . Comparisons between LPS group and LPS+PHPS1 group,  $**p < 0.01$ ; Comparisons between LPS+NAC group and LPS+PHPS1+NAC group,  $**p < 0.01$ ,  $*p < 0.05$ ,  $nsp > 0.05$ .

SHP2 has different physiological effects on different cells [28]. It has been found that it can inhibit the activity of Src protein by inhibiting the phosphorylation of Csk protein [29]. The activated Src protein plays an important role in promoting the activation of ERK [30]. In this study, by detecting p-SHP2, p-Src and p-ERK1/2 proteins in cardiomyocytes of mice in each group, we found that the expression of p-Src and p-ERK protein were lower than that in PHPS1 group. This result verified that SHP2 can inhibit the protein activity of Src and ERK.

ERK regulates NADPH oxidase-mediated Ros production [31]. P22, P47 and gp91, as components of NADPH oxidase, play an important role in the process of generating Ros [32]. In this study, the expression of P22, P47 and gp91 proteins in mouse cardiomyocytes was detected, and the expression of related proteins in model group was significantly lower than that in PHPS1 group, indicating that the mechanism of SHP2 improving myocardial injury in sepsis was to inhibit the expression of NADPH oxidase by inhibiting Src/ERK pathway, that is, to inhibit oxidative stress by inhibiting Src/ERK pathway.

Bax, Caspase-3, and Caspase-12 are all proteins involved in the process of apoptosis (programmed cell death). Bax is a member of the Bcl-2 family, a family of proteins that regulate apoptosis. The main function of BAX is to promote changes in the permeability of the outer mitochondrial membrane, thereby releasing pro-apoptotic factors such as cytochrome C within the cell and guiding the cell into the apoptotic pathway. Caspase-3 is a cysteine-specific cysteine protease that is a key executive enzyme in the apoptotic pathway. Once activated, caspase-3 can trigger the breakdown of a series

of proteins within the cell, leading to the rupture of cell membranes and the degradation of nucleic acids, ultimately promoting apoptosis. Caspase-12 is primarily involved in apoptosis induced by the endoplasmic reticulum stress pathway. Endoplasmic reticulum stress is a cellular stress response to abnormal endoplasmic reticulum and is usually activated when the endoplasmic reticulum is damaged. Activated caspase-12 can directly activate caspase-9 and caspase-3, thereby mediating apoptosis [33]. In this study, the expression of Bax, Caspase-3 and Caspase-12 protein in model group was significantly lower than that in the PHPS1 group. At the same time, the statistics of the number of apoptotic cells also confirmed that the number of apoptotic cardiomyocytes in model group was lower than that in PHPS1 group. Both of the results indicated that SHP2 inhibited the apoptosis of cardiomyocytes in myocardial injury caused by sepsis.

In the subsequent *in vitro* investigations, it was discerned that the expression of p-SHP2 protein diminished, while the expression of p-Src protein, proteins related to oxidative stress, and proteins related to apoptosis exhibited a notable increase subsequent to the introduction of PHPS1 to primary cardiomyocytes of neonatal mice. The expression of p-SHP2 protein, p-Src protein, proteins related to oxidative stress, and proteins related to apoptosis were suppressed following the administration of NAC, and the variance in the expression level of apoptosis-related proteins in cardiomyocytes exposed to the SHP2 inhibitor versus those treated with LPS was attenuated. NAC, recognized as the most extensively utilized antioxidant in experimental cell and animal biology, as well as clinical research, manifests a notable inhibitory influence on oxidative stress [34]. This outcome further corroborated the aforementioned experimental findings in the present study.

In summary, SHP2 alleviates sepsis-induced myocardial injury by impeding oxidative stress-mediated cardiomyocyte apoptosis through the Src/ERK pathway. SHP2 stands as a potential target for the clinical management of myocardial injury in sepsis.

## MATERIALS AND METHODS

### Groups and treatments

#### *Mice groups and mice model*

Eighteen 6-weeks-old SPF grade male C57BL/6J mice (C57BL/6JNifdc, Beijing Vital River Laboratory Animal Technology Co., Ltd., China) were reared adaptively for one week, during which all the mice had free access to food and water. One week later, the mice were randomly divided into sham group, model group and PHPS1 group, and each group consisted of 6 mice. The model of

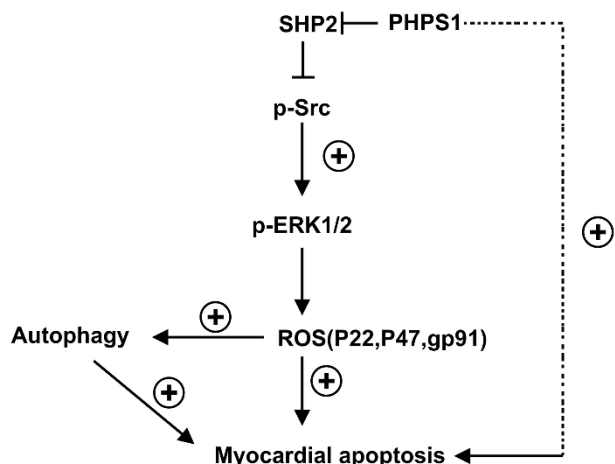


Figure 8. Schematic diagram of myocardial injury induced by SHP2 in sepsis.

myocardial injury induced by sepsis was established by intraperitoneal injection of LPS (20mg/kg) in the model group and the PHPS1 group. The mice in the sham group were given intraperitoneal injection of normal saline (20mg/kg). The mice in PHPS1 group were intraperitoneally injected with LPS and PHPS1(3 mg/kg) at the same time. The animal experiments in this study have been approved by the Medical Ethics Committee of Hebei General Hospital. Ethics Lot Number: 202376.

### ***Cells treatments and groups***

Five suckling C57BL/6 mice (J006), 1- 3 days old, were purchased from Nanjing Junke Bioengineering Co., Ltd. (China) After anesthesia, the suckling mice were disinfected with 75% ethanol. Under sterile conditions, the thoracic cavity of the mice was exposed with sterile ophthalmic scissors, and the hearts of the suckling mice were taken out and washed with PBS. The atrium and surrounding tissue vessels of suckling mice were stripped and washed again. The myocardial tissues were cut into tissue fragments of about 1mm<sup>3</sup> with ophthalmic scissors, and were lysed with lysis solution containing trypsin and type II collagenase. After lysis, the supernatant was centrifuged and obtained. Natural precipitation, discard the supernatant, add about 5ml of digestive solution, digest at 37° C for 20min (shake a few times every 2min), blow with a pipette for 1min, suck out the incomplete heart fragments into another centrifuge tube, add 2ml of cold culture medium to terminate digestion, 1000 rpm for 5min, discard the supernatant, add 2ml of D-Hanks solution to the precipitate, 1500 rpm for 10min, discard the supernatant, add 2ml of culture medium to the precipitate, and make a cell suspension by pipette. Then, the cells were cultured in DMEM medium (3-2010, Jiangsu CHI Scientific Biological Technology Co., Ltd.) containing 10% fetal bovine serum and 1% penicillin at 37° C with 5% CO<sub>2</sub>, and LPS, PHPS1((HY-112368, MedChem-Express, USA) and NAC (50303ES05, Yeasen Biotechnology (Shanghai, China) Co., Ltd.) were added into the medium respectively when the cell fusion reached 80%. Therefore, the cells were then divided into five groups: Group a (without LPS, PHPS1 or NAC), Group b (with LPS only), Group c (with LPS and PHPS1), Group d (with LPS and NAC) and Group e (with LPS, PHPS1 and NAC).

## **Methods**

### ***Echocardiogram detection***

The mice in each group were anesthetized with 50 mg/kg sodium pentobarbital, and the mice were observed after being given sodium pentobarbital, and the mice were kept until the mice were breathing steadily, their voluntary activities were reduced, their muscle tone was weakened, and the muscles were relaxed. Cardiac

ultrasound was examined with MX250 ultrasound probe under the Vevo3100 high-resolution small animal ultrasound imaging system, and the probe was placed in the short axis papillary muscle section of the left heart of the mouse to obtain M-mode echocardiography, the probe should not over compress the chest wall of the mouse, so as not to cause respiratory and cardiac arrest, and the ratio of the left ventricular ejection fraction (LVEF), left ventricular shortening fraction (LVFS) and E/A ratio were used to evaluate the changes in cardiac function in mice.

### ***HE staining***

After the mouse heart tissue was fixed in paraformaldehyde fixative solution for 48 hours, the sliced heart tissue was placed in an embedding box and placed in 4% paraformaldehyde fixative solution, and then dehydrated and transparent and sectioned. The thickness of the slice is 3-4  $\mu$ m. Place the slide rack containing tissue slides in a 60° C oven for 45 min, deparaffinize 2 times, 15 min each time, then pass through absolute ethanol for 10 seconds, 95% ethanol for 10 seconds, 80% ethanol for 10 seconds, and then wash the slides thoroughly with clean water for 1 time; Then the tissue was soaked in hematoxylin for 2 minutes, rinsed with tap water, differentiated with ethanol hydrochloride for 5 seconds, and returned to blue for 1 min; Then use eosin treatment for half a minute, rinse with tap water; Then dehydrate and use xylene transparently. The dehydrated transparent finished slides are placed in a fume hood to dry and neutral gum mounted, and the myocardial structure is observed under a microscope and photographed.

### ***Transmission electron microscope***

Hearts were taken from mice, washed with PBS, placed on an ice box, aspirated with a disposable dropper, and fixed with 2.5% glutaraldehyde solution. With 0.1 mol·L<sup>-1</sup> phosphate buffer, transfer the samples to 4° C and fix with 1% osmium acid for 3 h. With 0.1 mol·L<sup>-1</sup> phosphate buffer, samples were dehydrated with gradient ethanol: 30% ethanol for 15 min, 50% ethanol for 15 min, 70 ethanol uranyl acetate overnight, 80% ethanol for 15 min, 90% ethanol: 90% acetone (1:1) for 15 min (all steps were performed at 4° C), then treated with 100% acetone for 15 min  $\times$  3 h (room temperature), pure acetone + embedding solution (1:1) for 2 h (room temperature), pure embedding solution in a 37° C oven for 3 h. The samples were then embedded in the embedding solution in a 37° C oven for 12 h and in a pure embedding solution oven at 60° C for 48 h. Semi-thin sections with a thickness of 1  $\mu$ m were stained with sky blue and viewed under a light microscope to determine the location of the retina and the structure of the 10 layers. Ultrathin sections with a thickness of 80 nm were fished out, placed on a copper mesh of the supporting film, stained with lead citrate for 15 min,

washed 3 times with distilled water, dried naturally, and observed by transmission electron microscopy.

### **Western blot**

The cells were lysed with RIPA lysate (P0013K, Jiangsu Beyotime Biotechnology Co., Ltd., China). SDS-PAGE was used to analyze the protein, and after electrophoresis, the protein was transferred to PVDF membrane. Place the PVDF membrane into a TBST container packed with 5% skim milk and wash the membrane on a shaker for 10 min, pour out the TBST after 10 min, then add new TBST, wash the membrane again on the shaker for 10 min, pour out the TBST after 10 min, add clean TBST, and wash the membrane 3 times again on the shaker, then p-SHP2 antibody(ab62322, Abcam), p-Src antibody (ab40660, Abcam), p-ERK1/2 antibody (ab229912, Abcam), P22 antibody (ab75941, Abcam), P47 antibody (ab308256, Abcam), gp91 antibody (ab310337, Abcam), Bax antibody (ab32503, Abcam), Caspase-3 antibody (ab32351, Abcam), Caspase-12 antibody (ab62484, Abcam) and DAPDH antibody (ab8245, Abcam) were diluted in 1:1000 with TBST solution. After the washing is completed, the PVDF membrane is transferred to the HRP secondary antibody and incubated on a shaker for 2 hours at room temperature and in the dark. After the 2-hour secondary antibody incubation, wash the membrane again for 10 minutes each time, and develop color after the three times. Soak the membrane for 20 seconds using ECL chromogenic solution and develop color using a chemiluminescence imaging system, and the WB band of the protein of interest can be seen. Protein expression was measured by the gray value of the protein band.

### **TUNEL staining**

The heart tissue was deparaffinized with xylene, dehydrated with gradient ethanol, and 0.1% Triton X-100 was prepared with 0.1% sodium citrate, and then 50  $\mu$ l was added dropwise to each section, and then rinsed with PBS 3 times for 5 min each time after 8 min at room temperature. Enzyme solution and label solution were prepared 1:9 on ice to make TUNEL reaction. Wipe the specimen around it clean and add 50  $\mu$ l of TUNEL reaction dropwise. Incubate at 37° C with moisture and protection from light for 1 h, and then rinse the specimens with PBS for 3 times for 5 min each time. Add DAPI dropwise until the tissue is completely covered, and counterstain in the dark for 3 min. Rinse the specimen 3 times with PBS for 5 min each. The slices are removed and fluorescent quencher dropwise is added to seal the slices. Observe the staining effect under a microscope and take photos.

### **Statistical analysis**

All experiments in this study were repeated three times, and the data were statistically analyzed using SPSS 23.0

software. The measurement data was represented by ( $X\pm S$ ). The differences between two groups of data were tested by t-tests, and the differences among multiple groups were compared using one-way ANOVA.  $P<0.05$  was considered statistically significant.

## **AUTHOR CONTRIBUTIONS**

Jie Wang performed the experiments, analyzed the data, wrote the manuscript, designed the experiments. Qian Jia analyzed the data. Yu Zhang and Jing Li performed part of the TUNEL experiments.

## **CONFLICTS OF INTEREST**

The authors declare no conflicts of interest.

## **ETHICAL STATEMENT**

The animal experiments in this study have been approved by the Medical Ethics Committee of Hebei General Hospital. Ethics Lot Number: 202376.

## **FUNDING**

This study was supported by the 2022 Medical Science Research Project of Hebei Provincial Health and Health Commission (No.20220929).

## **REFERENCES**

1. Arina P, Singer M. Pathophysiology of sepsis. *Curr Opin Anaesthesiol.* 2021; 34:77–84.  
<https://doi.org/10.1097/ACO.0000000000000963>  
PMID:[33652454](https://pubmed.ncbi.nlm.nih.gov/33652454/)
2. Huang M, Cai S, Su J. The Pathogenesis of Sepsis and Potential Therapeutic Targets. *Int J Mol Sci.* 2019; 20:5376.  
<https://doi.org/10.3390/ijms20215376>  
PMID:[31671729](https://pubmed.ncbi.nlm.nih.gov/31671729/)
3. Chu M, Qian L, Zhu M, Yao J, Xu D, Chen M. Circumferential strain rate to detect lipopolysaccharide-induced cardiac dysfunction: a speckle tracking echocardiography study. *Quant Imaging Med Surg.* 2019; 9:151–9.  
<https://doi.org/10.21037/qims.2018.11.03>  
PMID:[30976539](https://pubmed.ncbi.nlm.nih.gov/30976539/)
4. Ge C, Liu J, Dong S. miRNA-214 Protects Sepsis-Induced Myocardial Injury. *Shock.* 2018; 50:112–8.  
<https://doi.org/10.1097/SHK.0000000000000978>  
PMID:[28858140](https://pubmed.ncbi.nlm.nih.gov/28858140/)
5. Liu YC, Yu MM, Shou ST, Chai YF. Sepsis-Induced Cardiomyopathy: Mechanisms and Treatments. *Front Immunol.* 2017; 8:1021.

- <https://doi.org/10.3389/fimmu.2017.01021>  
PMID:[28970829](https://pubmed.ncbi.nlm.nih.gov/28970829/)
6. Zhu H, Zhang L, Jia H, Xu L, Cao Y, Zhai M, Li K, Xia L, Jiang L, Li X, Zhou Y, Liu J, Yu S, Duan W. Tetrahydrocurcumin improves lipopolysaccharide-induced myocardial dysfunction by inhibiting oxidative stress and inflammation via JNK/ERK signaling pathway regulation. *Phytomedicine*. 2022; 104:154283. <https://doi.org/10.1016/j.phymed.2022.154283> PMID:[35779282](https://pubmed.ncbi.nlm.nih.gov/35779282/)
  7. Stanzani G, Duchon MR, Singer M. The role of mitochondria in sepsis-induced cardiomyopathy. *Biochim Biophys Acta Mol Basis Dis*. 2019; 1865:759–73. <https://doi.org/10.1016/j.bbadis.2018.10.011> PMID:[30342158](https://pubmed.ncbi.nlm.nih.gov/30342158/)
  8. Peoples JN, Saraf A, Ghazal N, Pham TT, Kwong JQ. Mitochondrial dysfunction and oxidative stress in heart disease. *Exp Mol Med*. 2019; 51:1–13. <https://doi.org/10.1038/s12276-019-0355-7> PMID:[31857574](https://pubmed.ncbi.nlm.nih.gov/31857574/)
  9. Xin T, Lu C. SirT3 activates AMPK-related mitochondrial biogenesis and ameliorates sepsis-induced myocardial injury. *Aging (Albany NY)*. 2020; 12:16224–37. <https://doi.org/10.18632/aging.103644> PMID:[32721927](https://pubmed.ncbi.nlm.nih.gov/32721927/)
  10. Tan Y, Ouyang H, Xiao X, Zhong J, Dong M. Irisin ameliorates septic cardiomyopathy via inhibiting DRP1-related mitochondrial fission and normalizing the JNK-LATS2 signaling pathway. *Cell Stress Chaperones*. 2019; 24:595–608. <https://doi.org/10.1007/s12192-019-00992-2> PMID:[30993599](https://pubmed.ncbi.nlm.nih.gov/30993599/)
  11. Kanumuri R, Kumar Pasupuleti S, Burns SS, Ramdas B, Kapur R. Targeting SHP2 phosphatase in hematological malignancies. *Expert Opin Ther Targets*. 2022; 26:319–32. <https://doi.org/10.1080/14728222.2022.2066518> PMID:[35503226](https://pubmed.ncbi.nlm.nih.gov/35503226/)
  12. Song Z, Wang M, Ge Y, Chen XP, Xu Z, Sun Y, Xiong XF. Tyrosine phosphatase SHP2 inhibitors in tumor-targeted therapies. *Acta Pharm Sin B*. 2021; 11:13–29. <https://doi.org/10.1016/j.apsb.2020.07.010> PMID:[33532178](https://pubmed.ncbi.nlm.nih.gov/33532178/)
  13. Heun Y, Pircher J, Czermak T, Bluem P, Hupel G, Bohmer M, Kraemer BF, Pogoda K, Pfeifer A, Woernle M, Ribeiro A, Hübner M, Kreth S, et al. Inactivation of the tyrosine phosphatase SHP-2 drives vascular dysfunction in Sepsis. *EBioMedicine*. 2019; 42:120–32. <https://doi.org/10.1016/j.ebiom.2019.03.034> PMID:[30905847](https://pubmed.ncbi.nlm.nih.gov/30905847/)
  14. Dong F, Li H, Liu L, Yao LL, Wang J, Xiang D, Ma J, Zhang G, Zhang S, Li J, Jiang SH, Hu X, Chen J, Bao Z. ACE2 negatively regulates the Warburg effect and suppresses hepatocellular carcinoma progression via reducing ROS-HIF1 $\alpha$  activity. *Int J Biol Sci*. 2023; 19:2613–29. <https://doi.org/10.7150/ijbs.81498> PMID:[37215979](https://pubmed.ncbi.nlm.nih.gov/37215979/)
  15. Jiang J, Hu B, Chung CS, Chen Y, Zhang Y, Tindal EW, Li J, Ayala A. SHP2 inhibitor PHS1 ameliorates acute kidney injury by Erk1/2-STAT3 signaling in a combined murine hemorrhage followed by septic challenge model. *Mol Med*. 2020; 26:89. <https://doi.org/10.1186/s10020-020-00210-1> PMID:[32957908](https://pubmed.ncbi.nlm.nih.gov/32957908/)
  16. Ye S, Zuo B, Xu L, Wu Y, Luo R, Ma L, Yao W, Chen L, Liang G, Zhang Y. Inhibition of SHP2 by the Small Molecule Drug SHP099 Prevents Lipopolysaccharide-Induced Acute Lung Injury in Mice. *Inflammation*. 2023; 46:975–86. <https://doi.org/10.1007/s10753-023-01784-8> PMID:[36732395](https://pubmed.ncbi.nlm.nih.gov/36732395/)
  17. Xu Z, Guo C, Ye Q, Shi Y, Sun Y, Zhang J, Huang J, Huang Y, Zeng C, Zhang X, Ke Y, Cheng H. Endothelial deletion of SHP2 suppresses tumor angiogenesis and promotes vascular normalization. *Nat Commun*. 2021; 12:6310. <https://doi.org/10.1038/s41467-021-26697-8> PMID:[34728626](https://pubmed.ncbi.nlm.nih.gov/34728626/)
  18. Dai S, Ye B, Zhong L, Chen Y, Hong G, Zhao G, Su L, Lu Z. GSDMD Mediates LPS-Induced Septic Myocardial Dysfunction by Regulating ROS-dependent NLRP3 Inflammasome Activation. *Front Cell Dev Biol*. 2021; 9:779432. <https://doi.org/10.3389/fcell.2021.779432> PMID:[34820388](https://pubmed.ncbi.nlm.nih.gov/34820388/)
  19. Hollenberg SM, Singer M. Pathophysiology of sepsis-induced cardiomyopathy. *Nat Rev Cardiol*. 2021; 18:424–34. <https://doi.org/10.1038/s41569-020-00492-2> PMID:[33473203](https://pubmed.ncbi.nlm.nih.gov/33473203/)
  20. L'Heureux M, Sternberg M, Brath L, Turlington J, Kashiouris MG. Sepsis-Induced Cardiomyopathy: a Comprehensive Review. *Curr Cardiol Rep*. 2020; 22:35. <https://doi.org/10.1007/s11886-020-01277-2> PMID:[32377972](https://pubmed.ncbi.nlm.nih.gov/32377972/)
  21. Qiu J, Xiao X, Gao X, Zhang Y. Ulinastatin protects against sepsis-induced myocardial injury by inhibiting NLRP3 inflammasome activation. *Mol Med Rep*. 2021; 24:730. <https://doi.org/10.3892/mmr.2021.12369> PMID:[34414461](https://pubmed.ncbi.nlm.nih.gov/34414461/)
  22. Deng C, Liu Q, Zhao H, Qian L, Lei W, Yang W, Liang Z, Tian Y, Zhang S, Wang C, Chen Y, Yang Y. Activation of

- NR1H3 attenuates the severity of septic myocardial injury by inhibiting NLRP3 inflammasome. *Bioeng Transl Med.* 2023; 8:e10517.  
<https://doi.org/10.1002/btm2.10517> PMID:[37206244](https://pubmed.ncbi.nlm.nih.gov/37206244/)
23. Fu W, Fang X, Wu L, Hu W, Yang T. Neogambogic acid relieves myocardial injury induced by sepsis *via* p38 MAPK/NF- $\kappa$ B pathway. *Korean J Physiol Pharmacol.* 2022; 26:511–8.  
<https://doi.org/10.4196/kjpp.2022.26.6.511> PMID:[36302625](https://pubmed.ncbi.nlm.nih.gov/36302625/)
  24. Zhu Y, Wu Z, Yan W, Shao F, Ke B, Jiang X, Gao J, Guo W, Lai Y, Ma H, Chen D, Xu Q, Sun Y. Allosteric inhibition of SHP2 uncovers aberrant TLR7 trafficking in aggravating psoriasis. *EMBO Mol Med.* 2022; 14:e14455.  
<https://doi.org/10.15252/emmm.202114455> PMID:[34936223](https://pubmed.ncbi.nlm.nih.gov/34936223/)
  25. Qi C, Han T, Tang H, Huang K, Min J, Li J, Ding X, Xu Z. Shp2 Inhibits Proliferation of Esophageal Squamous Cell Cancer via Dephosphorylation of Stat3. *Int J Mol Sci.* 2017; 18:134.  
<https://doi.org/10.3390/ijms18010134> PMID:[28085101](https://pubmed.ncbi.nlm.nih.gov/28085101/)
  26. Chen J, Cao Z, Guan J. SHP2 inhibitor PHP51 protects against atherosclerosis by inhibiting smooth muscle cell proliferation. *BMC Cardiovasc Disord.* 2018; 18:72.  
<https://doi.org/10.1186/s12872-018-0816-2> PMID:[29703160](https://pubmed.ncbi.nlm.nih.gov/29703160/)
  27. Su LJ, Zhang JH, Gomez H, Murugan R, Hong X, Xu D, Jiang F, Peng ZY. Reactive Oxygen Species-Induced Lipid Peroxidation in Apoptosis, Autophagy, and Ferroptosis. *Oxid Med Cell Longev.* 2019; 2019:5080843.  
<https://doi.org/10.1155/2019/5080843> PMID:[31737171](https://pubmed.ncbi.nlm.nih.gov/31737171/)
  28. Chang CJ, Lin CF, Chen BC, Lin PY, Chen CL. SHP2: The protein tyrosine phosphatase involved in chronic pulmonary inflammation and fibrosis. *IUBMB Life.* 2022; 74:131–42.  
<https://doi.org/10.1002/iub.2559> PMID:[34590785](https://pubmed.ncbi.nlm.nih.gov/34590785/)
  29. Kong J, Long YQ. Recent advances in the discovery of protein tyrosine phosphatase SHP2 inhibitors. *RSC Med Chem.* 2022; 13:246–57.  
<https://doi.org/10.1039/d1md00386k> PMID:[35434626](https://pubmed.ncbi.nlm.nih.gov/35434626/)
  30. Wang Q, Chang H, Shen Q, Li Y, Xing D. Photobiomodulation therapy for thrombocytopenia by upregulating thrombopoietin expression via the ROS-dependent Src/ERK/STAT3 signaling pathway. *J Thromb Haemost.* 2021; 19:2029–43.  
<https://doi.org/10.1111/jth.15252> PMID:[33501731](https://pubmed.ncbi.nlm.nih.gov/33501731/)
  31. Yasuoka H, Garrett SM, Nguyen XX, Artlett CM, Feghali-Bostwick CA. NADPH oxidase-mediated induction of reactive oxygen species and extracellular matrix deposition by insulin-like growth factor binding protein-5. *Am J Physiol Lung Cell Mol Physiol.* 2019; 316:L644–55.  
<https://doi.org/10.1152/ajplung.00106.2018> PMID:[30810066](https://pubmed.ncbi.nlm.nih.gov/30810066/)
  32. Sadri S, Tomar N, Yang C, Audi SH, Cowley AW, Dash RK. Mechanistic computational modeling of the kinetics and regulation of NADPH oxidase 2 assembly and activation facilitating superoxide production. *Free Radic Res.* 2020; 54:695–721.  
<https://doi.org/10.1080/10715762.2020.1836368> PMID:[33059489](https://pubmed.ncbi.nlm.nih.gov/33059489/)
  33. Guo MM, Qu SB, Lu HL, Wang WB, He ML, Su JL, Chen J, Wang Y. Biochanin A Alleviates Cerebral Ischemia/Reperfusion Injury by Suppressing Endoplasmic Reticulum Stress-Induced Apoptosis and p38MAPK Signaling Pathway *In Vivo* and *In Vitro*. *Front Endocrinol (Lausanne).* 2021; 12:646720.  
<https://doi.org/10.3389/fendo.2021.646720> PMID:[34322090](https://pubmed.ncbi.nlm.nih.gov/34322090/)
  34. Pedre B, Barayeu U, Ezeriņa D, Dick TP. The mechanism of action of N-acetylcysteine (NAC): The emerging role of H<sub>2</sub>S and sulfane sulfur species. *Pharmacol Ther.* 2021; 228:107916.  
<https://doi.org/10.1016/j.pharmthera.2021.107916> PMID:[34171332](https://pubmed.ncbi.nlm.nih.gov/34171332/)